Biochemical and Biophysical Research Communications 527 (2020) 365–371

Contents lists available at ScienceDirect

Biochemical and Biophysical Research Communications

journal homepage: www.elsevier.com/locate/ybbrc

Effect of methionine/choline-deficient diet and high-fat diet-induced steatohepatitis on mitochondrial homeostasis in mice

Yoshihisa Arao [a], Hirokazu Kawai [a, *], Kenya Kamimura [a], Takamasa Kobayashi [a], Oki Nakano [a], Manabu Hayatsu [b], Tatsuo Ushiki [b], Shuji Terai [a]

[a] Division of Gastroenterology and Hepatology, Niigata University Graduate School of Medical and Dental Sciences, Niigata, Japan
[b] Division of Microscopic Anatomy, Niigata University Graduate School of Medical and Dental Sciences, Niigata, Japan

ARTICLE INFO

Article history:
Received 13 March 2020
Accepted 30 March 2020
Available online 10 April 2020

Keywords:
Methionine/choline-deficient diet
High-fat diet
Mitochondrial biogenesis
Mitochondrial degradation
Mitochondrial DNA copy Number
Oxidative stress

ABSTRACT

Considering the increase in cases of non-alcoholic steatohepatitis (NASH), the use of appropriate animal model of NASH is essential to understand the underlying pathogenesis mechanism. To date, several mice models have been used; however, significant differences in the etiologies and food administered affected the results, with inconsistent conclusions. Therefore, it is necessary to understand these models and their differences to be able to choose appropriate models. Inspired by the fact that mitochondrial (mt)DNA content is changed in non-alcoholic fatty liver disease in humans, we investigated the mtDNA copy number in the NASH mice models induced by high-fat diet (HFD) and methionine/choline-deficient diet (MCD) to understand the differences between these models. Megamitochondria were observed in both MCD and HFD groups. However, the MCD group showed significant decrease in liver mtDNA content compared with that in the HFD group. These changes were associated with significant upregulation of mitochondrial biogenesis- and degradation-related genes in MCD model than in HFD model. Thus, stability of mtDNA is associated with the differences between MCD and HFD-induced NASH models often used in studies; these findings could help in choosing appropriate models for studies on NASH.

1. Introduction

There has been a rise in morbidity due to non-alcoholic fatty liver disease (NAFLD), including non-alcoholic steatohepatitis (NASH). In addition, there is high variability of disease conditions, including the clinical course, etiology, metabolic status, and histological changes. Hence, research using appropriate mice models has become essential. To date, mouse models fed methionine/choline-deficient diet (MCD)- and high-fat diet (HFD) have been used to study the disease. However, these models have been chosen in previous NASH-related studies with no consideration on the significant difference in their etiology, mechanisms, and changes in the liver and therefore, lead to inconsistent results in the similar design studies. For example, while HFD-fed model showed poorer insulin sensitivity [1], MCD-fed model showed better insulin sensitivity [2]. Furthermore, the histological changes in the liver is reversible when HFD is removed from the HFD-fed model, while MCD-fed model shows no reversibility in its histological conditions [3]. Hence, there is a need to further understand these models to be able to accurately draw conclusions. To determine the differences in these mice models we focused on the condition of mitochondria, as oxidative stress-induced mitochondrial dysfunction is reported to be one of the pathogenesis mechanisms of NASH [4]. As mitochondrial DNA (mtDNA) lacks histones, it is vulnerable to ROS, leading to DNA copy number changes [5]. To date, the mtDNA copy number have been reported to change in various diseases, including heart failure, diabetes, and malignancies [6–8]. However, few studies have measured mtDNA copy numbers in liver tissues in patients with NAFLD and reported inconsistent results [9–12]. Considering that results of these studies could be affected by individual variability in the etiologies and histological changes, in the current study, we focused on changes in mtDNA copy number in MCD- and HFD-fed mice NASH models. MCD triggered dietary steatohepatitis and HFD triggered only accumulation of fat generically without fibrosis. We also included a dietary recovery group, wherein mice were returned to control diet after HFD. We assessed liver mtDNA copy numbers by real-time polymerase chain reaction (RT-PCR) and mitochondrial biogenesis/degradation by

* Corresponding author. Division of Internal Medicine, Niigata Prefectural Shibata Hospital, Shibata, 1-2-8 Honcho, Shibata, Niigata, 957-8588, Japan.
E-mail address: kawaih@med.niigata-u.ac.jp (H. Kawai).

https://doi.org/10.1016/j.bbrc.2020.03.180
0006-291X/

quantitative RT-PCR (RT-qPCR) and western blotting. In addition, ROS increase by the metabolization of accumulated triglycerides (TGs) in the liver via mitochondrial and peroxisomal oxidation was assessed using 8-hydroxy-2′-deoxyguanosine (8-OHdG).

2. Materials and methods

2.1. Animals

Six-week-old male C56BL/6 N mice were purchased from Charles River Japan (Yokohama, Japan). All mice were housed under specific pathogen-free conditions in a temperature-controlled animal facility with a 12-h light/dark cycle and had free access to food and water. Body weights were measured weekly. Mice were fed a standard chow or HFD (HFD32; 507.6 kcal/100 g, 56.7% energy as fat, 20.1% protein, and 23.1% carbohydrates; CLEA Japan, Tokyo, Japan) [13] and were defined as a Chow group or HFD group, respectively. To induce steatohepatitis, MCD (A02082002B; 424.7 kcal/100 g, 21.2% energy as fat, 16.1% protein, and 62.7% carbohydrates; Research Diets, Inc., New Brunswick, NJ, USA) [14] was used. Mice in the Chow, HFD, and MCD groups were euthanized after feeding for 2, 6, or 10 weeks. Some mice were fed HFD for 6 weeks and standard chow for the subsequent 4 weeks and were defined as the recovery (HFD-R) group. Liver tissues were collected and snap-frozen in liquid nitrogen, and sera were obtained from collected blood. Liver tissues were fixed in formalin and embedded in paraffin for histological analysis. Fasting blood glucose levels were measured using a Glutest Neo Super (Sanwa Kagaku Kenkyusho Co., Ltd., Nagoya, Japan). Serum levels of alanine aminotransferase (ALT) and TGs were measured by enzyme-linked immunosorbent assays (Oriental Yeast Co., Nagahama, Japan).

All protocols and procedures were in accordance with The Code of Ethics of the World Medical Association (Declaration of Helsinki), Uniform Requirements for manuscripts submitted to Biomedical journals, the guidelines of the Niigata University Committee for the Care and Use of Laboratory Animals, and were approved by the Animal Experiments Ethics Committee of Niigata University (approval number 178-2).

2.2. Histological analysis

Liver sections were stained with hematoxylin and eosin (H&E) and Sirius red. Fibrotic areas, stained with Sirius red, were measured using BZ-X 700 imaging software (Keyence, Osaka, Japan) in five distinct microscopic fields.

Transmission electron microscopy (TEM) was used for morphologic assessment. For TEM, fresh small tissue blocks from the liver were fixed with 2.0% glutaraldehyde in 0.1 mol/L phosphate buffer (pH 7.4). The specimens were post-fixed in 1% osmium tetroxide. The material was then dehydrated through a graded series of ethanol concentrations and propylene oxide, embedded in epoxy resin, and sectioned using an Ultracut-N ultramicrotome (Reichert, Vienna, Austria) into ultrathin sections (70 nm). Sections were double-stained with uranyl acetate and lead citrate and examined under an H-7650 transmission electron microscope (Hitachi, Tokyo, Japan).

2.3. Determination of liver and muscle mtDNA copy numbers

Genomic DNA was extracted from liver samples using the DNeasy blood and tissue kit (Qiagen, Hilden, Germany) according to the manufacturer's instructions, and mtDNA copy numbers were measured by absolute quantification using real-time PCR. Mitochondrial NADH-ubiquinone oxidoreductase chain 1 (*Nd1*) and nuclear β-actin (*Actb*) genes were cloned into the pGEM-T vector (Promega, Madison, WI, USA), and serial dilutions of resulting plasmids were used to obtain standard curves by real-time PCR. The concentrations of *Nd1* and *Actb* in sample tissues were determined by real-time PCR using the corresponding standard curves and converted to copy numbers. The copy number of mtDNA per nuclear DNA was calculated by dividing the *Nd1* copy number by that of *Actb*. Real-time PCR was performed in triplicate with TaqMan primers (Applied Biosystems, Foster City, CA, USA) using a StepOne Plus system (Applied Biosystems). The thermal cycling conditions were 50 °C for 2 min and 95 °C for 10 min, followed by 40 cycles of 95 °C for 15 s and 60 °C for 1 min. PCR amplification was carried out in a 96-well plate, with negative and positive controls and a standard curve series included in each run.

2.4. RT-qPCR

Total RNA was extracted from liver tissue with the RNeasy kit (Qiagen) and converted into cDNA using a first-strand cDNA synthesis kit (TaKaRa, Shiga, Japan). Specific gene expression was quantified by RT-qPCR using SYBR Green and the StepOne Plus system, and the results were analyzed with the bundled software. The following genes were assessed: peroxisome proliferator-activated receptor gamma coactivator 1-alpha (*Ppargc1a*), transcription factor A (*Tfam*), nuclear respiratory factor 1 (*Nrf1*), *Nrf2*, microtubule-associated protein 1A/1B-light chain 3 beta (*Lc3b*), parkin (*Prkn*), PTEN-induced putative kinase 1 (*Pink1*), Kelch-like ECH-associated protein 1 (*Keap1*), and glyceraldehyde 3-phosphate dehydrogenase (*Gapdh*). Primer sequences are shown in Supplementary Table 1. The thermal conditions were as follows: 95 °C for 10 min, followed by 40 cycles of 95 °C for 15 s and 60 °C for 1 min, with the PCR product melting hold at 95 °C for 15 s, 60 °C for 1 min, and 95 °C for 15 s. Changes in gene expression were evaluated using the $2^{-\Delta\Delta Ct}$ method, with gene expression normalized to that of *Gapdh* in each sample.

2.5. Western blotting

Tissues were homogenized and sonicated in sample buffer. Equivalent amounts of protein for each group were run on sodium dodecyl sulfate polyacrylamide gels. Proteins were electrotransferred to polyvinylidene difluoride membranes, which were incubated with antibodies against PGC-1α, (NBP1-04676, 1:500, Novus Biologicals, Littleton, CO, USA), LC3B (#2775, 1:200, Cell Signaling Technology, Danvers, MA, USA), and GAPDH (#2118, 1:200, Cell Signaling Technology). Membranes were washed and incubated with secondary antibodies of antirabbit (NA9340V, GE Healthcare, Little Chalfont, Buckinghamshire, UK) antibody conjugated with horseradish peroxidase. Protein bands were visualized using Amersham ECL Prime Western Blotting Detection Reagent (GE Healthcare), with GAPDH used as a loading control.

2.6. Immunofluorescence of 8-OHdG

Liver samples were fixed in 10% formaldehyde and incubated with primary antibody against 8-OHdG (ab10802, 1:400, Abcam, Tokyo, Japan) at 4 °C overnight, followed by incubation with secondary antibody (AK-5005, Vector Laboratories, Burlington, Canada) and fluorescent dye conjugates (Alexa Fluor 555, 1:200, Life Technologies, Carlsbad, CA, USA). Immunofluorescence intensity was quantified in five randomly selected areas per specimen using BZ-X 700 imaging software (Keyence).

2.7. Statistical analysis

Statistical analysis was done using GraphPad Prism version 7

(GraphPad Software Inc., California, USA). Results are expressed as means ± standard deviation. Intergroup comparison was done by factorial analysis of variance (ANOVA) followed by *post hoc* Tukey's test, if data were normally distributed, or by Kruskal ANOVA followed by Dunn's test if data were skewed. Differences were considered statistically significant at $p < 0.05$.

3. Results

3.1. Changes in mtDNA copy numbers in liver and expression of genes related to mitochondrial biogenesis/degradation

The HFD-fed mice showed high level of mtDNA copy numbers of 11,190 ± 3,346, 13,047 ± 3,308, and 12,288 ± 1,325 after 2, 6, and 10 weeks, respectively, but was not significantly different from that in control diet-fed mice showing 10,690 ± 1,811, 10,692 ± 3,481, and 8,489 ± 1,870 at the same time-points (Fig. 1A). In contrast, MCD-fed mice showed significantly lower mtDNA copy numbers of 6,633 ± 250, 6,417 ± 1,979 ($p < 0.01$), and 5,961 ± 1,642 ($p < 0.01$) at the same time-points. To determine the stability of the mitochondria, we examined the expression of the mitochondrial biogenesis-related genes *Ppargc1a*, *Tfam*, *Nrf1*, *Nrf2*, and *Keap1* and degradation-related genes *LC3B*, *Parkin*, and *Pink*. While HFD-fed group showed inhibition of *Tfam*, *Parkin*, and *Pink1* gene expression, MCD-fed group showed significant activation of both biogenesis-related genes (*Ppargc1a, Tfam, Nrf1, Nrf2, Keap1*) and degradation-related genes at 10 weeks (*LC3B* and *Pink1*) ($p < 0.01$, Fig. 1B). The time-dependent changes in expression of LC3B at six weeks showed consistent results with the gene expression levels in the liver of mice groups (Fig. 1C). These results suggested that the level of mtDNA is maintained in HFD-fed mice and is decreased in MCD-fed mice due to the higher level of mitochondrial turnover.

3.2. Oxidative DNA damage in liver

To determine whether the oxidative stress induced by MCD and HFD affected the mtDNA copy number in the hepatocytes, the levels of 8-OHdG, a marker of oxidative nucleic acid damage, were quantified in the models (Fig. 1D and E). At 10 weeks of treatment, both MCD and HFD-fed mice showed significantly higher levels of 8-OHdG expression than those in chow diet-fed mice (mean brightness integration value in MCD, 2.04; HFD, 2.79; Chow, 0.25, $p < 0.05$). These results indicated that there were no clear correlations between diet-induced ROS and mtDNA copy numbers. To confirm the reversibility of the effect of diet-induced ROS, changes in 8-OHdG expression was checked in HFD-R group, which was fed with HFD for 6 weeks followed by 4 weeks of chow diet. Notably, the 8-OHdG level in the HFD-R group significantly reduced and recovered to that in the control group, and was significantly lower than that in MCD- and HFD-fed mice ($p < 0.01$). These results suggest that diet-induced accumulation of ROS is reversible in HFD.

3.3. Effect of MCD and HFD on hepatic tissue and ultrastructure of mitochondria in liver

Histological analysis of the liver after H&E staining (Fig. 2A and D) showed that steatosis, observed as lipid macro- and microvesicles, increased in the HFD group (Fig. 2C) and infiltration of inflammatory cells in the liver, in addition to steatosis, was seen in MCD-fed mice (Fig. 2B). Importantly, fat accumulation in the liver remarkably decreased to the same level as that in the Chow group in the HFD-R group (Fig. 2D), evidenced by the quantification of the fat tissue in the liver (Fig. 2E). Sirius red staining of liver tissues (Fig. 2F–I) demonstrated that fibrotic areas significantly increased in the MCD group than that in the chow- and HFD-fed mice (Fig. 2J).

In hepatocytes, TEM frequently revealed megamitochondria with abnormally irregular shapes in the HFD and MCD groups (Fig. 2L, M). Megamitochondria persisted in the HFD-R group, despite considerable reduction in steatosis (Fig. 2N).

Together, these results suggest that the HFD has relatively stronger fat-accumulating effects in the liver, while MCD has stronger fibrosis-inducing effects. Moreover, the fatty tissue can be reversible in HFD.

3.4. Effects of the diets on body weight and biochemical test results

The body weight increased across the weeks in the HFD. In contrast, it did not increase in the MCD group, which showed significantly lower body weights compared with that in the Chow and HFD groups at each time point. In the HFD-R group, the body weight decreased to a level (35.9 ± 0.7 g) comparable to that in the Chow group (31.0 ± 2.5 g) at 10 weeks (Fig. 3A). The fasting blood glucose level was also lower in the MCD than in the HFD group at each time point (Fig. 3B). The ALT levels increased across the weeks in the MCD group (2 weeks, 409.8 ± 168.4 IU/L; 6 weeks, 550.5 ± 252.1 IU/L; 10 weeks, 976 ± 413.3 IU/L) and was notably higher than that in the Chow and HFD group at each time point (Fig. 3C). In the HFD-R group, the fasting blood glucose and ALT did not change, and was comparable to that in the HFD group at 10 weeks. Serum TG levels did not significantly change in any group, except for an increase in the MCD group at 6 weeks (Fig. 3D). These results suggest that MCD showed higher hepatic toxicity with body weight loss and hypoglycemia, while HFD is related to the reversible and milder hepatotoxicity and body weight gain.

4. Discussion

Our results demonstrated significant differences in the mtDNA copy number between MCD- and HFD-induced NASH, which may be related to the differences in the mice models and might also be associated with differences in individual patients. This was further reflected by the fact that the HFD group showed increasing body weight with time and fat accumulation without fibrosis, while the MCD group showed lower body weight, steatohepatitis with fibrosis, and increasing serum ALT levels compared to the HFD group. In addition, recovery from HFD (HFD-R) showed improvement in the body weight and fat accumulation. Notably, MCD group showed lower mtDNA copy number than HFD group, and this might be due to the higher rate of mitochondrial turnover in the MCD mice, as evidenced by the upregulation of both mitochondrial biogenesis and degradation-related genes. These findings may reflect the differences in human NAFLD disease types, which show significant variations in each individual and inconsistent results regarding the mtDNA copy number in human liver steatosis, if the differences in pathophysiological conditions of subjects, etiologies, and other conditions are not considered [9–12]. Predominance of fatty liver in subjects can lead to a higher average mtDNA copy number [9,10]. Conversely, a high proportion of steatohepatitis subjects show reduced copy numbers [11,12].

Considering the results that HFD-fed mice showed recovery of the disease status with mtDNA copy numbers similar to that observed in the chow-fed mice, and MCD-fed mice showed consistently lower number of mtDNA with no reversibility [3], reversibility of mtDNA copy numbers may reflect the disease conditions of human steatohepatitis. Therefore, mtDNA copy number can be a biomarker of clinical state of NASH in the future. In addition, 8-OHdG levels could be recovered in HFD-fed mice, indicating ROS reduction by the specific diet [15]. Some damaged mitochondria, however, may remain in hepatocytes for a prolonged period, even after alleviation of fat accumulation in the liver.

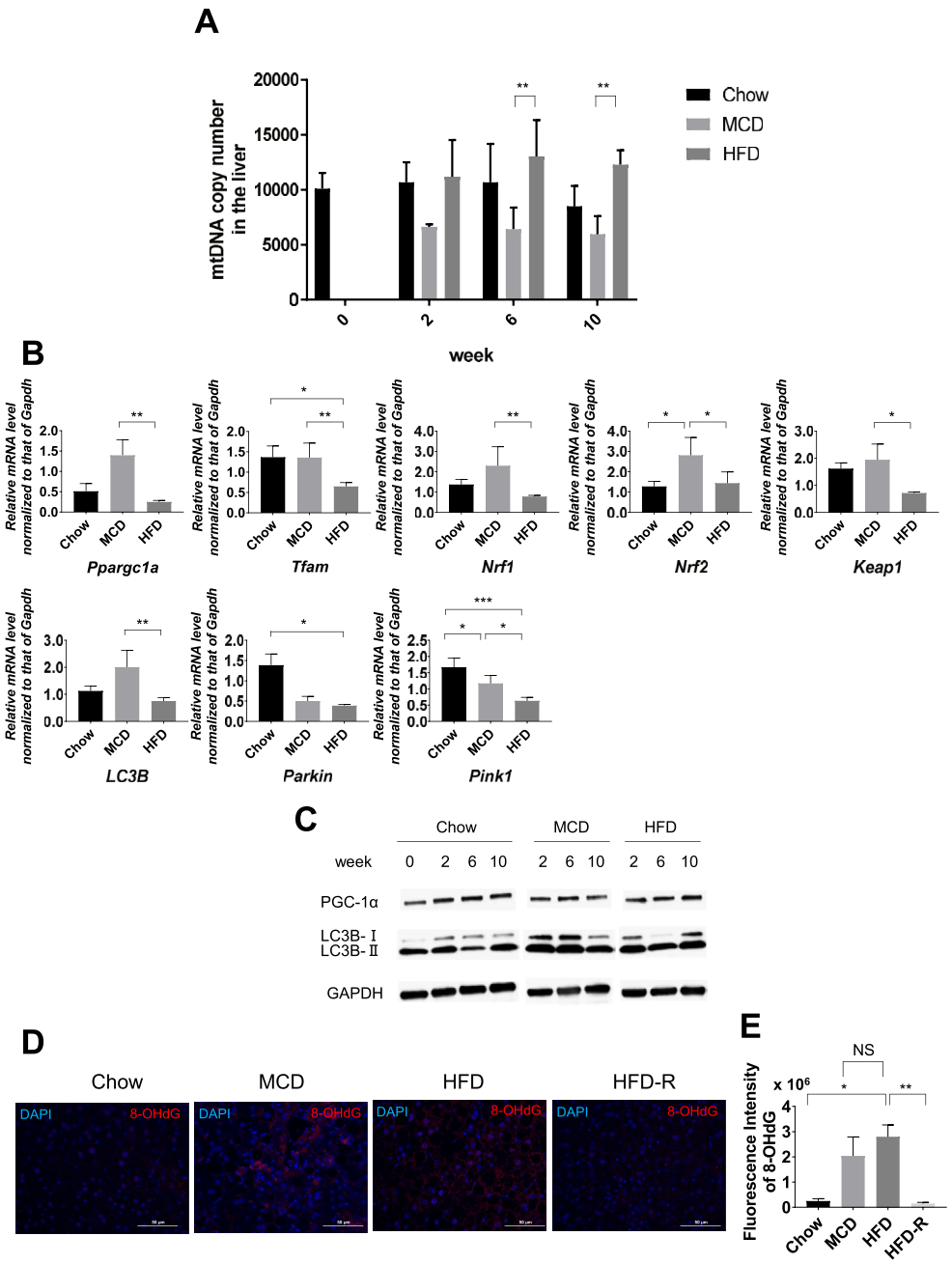

Fig. 1. mtDNA copy numbers in the liver, mitochondria biogenesis/degradation-related gene expression and protein level, and immunofluorescence staining of 8-OHdG
(A) mtDNA copy numbers in the liver. (B) Expression of mitochondrial biogenesis- and degradation-related genes. *Gapdh* was used as an internal control. (C) Protein expression levels, measured by western blotting, in the livers of mice fed different diets for 10 weeks. (D) Representative liver sections after immunofluorescence staining for 8-OHdG in the liver. Magnification, 400 × . (E) Quantification of immunofluorescence intensity of 8-OHdG. Results are presented as the means ± SD. *$p < 0.05$, **$p < 0.01$, ***$p < 0.001$. Images are representative of five independent experiments. For mtDNA copy number, intergroup comparison was done by two-way factorial ANOVA followed by Tukey's test. For analysis of *Tfam*, *Nrf2*, and *Pink1* expression, intergroup comparison was done by factorial ANOVA followed by Tukey's test. For analysis of *Ppargc*, *Nrf1*, *Keap1*, *LC3B*, *parkin*, and 8-OHdG, intergroup comparison was done by Kruskal Wallis ANOVA followed by Dunn's test.
Abbreviations: MCD, methionine/choline-deficient diet; HFD, high-fat diet; NS, Not Significant; DAPI, 4′,6-diamidino-2-phenylindole. . (For interpretation of the references to colour in this figure legend, the reader is referred to the Web version of this article.)

To our knowledge, the current study demonstrates for the first time, correlations between changes in mtDNA copy numbers in the liver and dietary changes. Perrone et al. [16] investigated gene and protein expression and mtDNA copy numbers in liver of rats fed a methionine-restricted (MR) diet, which induced resistance to adiposity. Although mitochondrial aerobic capacity was enhanced in the liver of the MR rats, mtDNA content was unaltered in these tissues. In this study, the reason for the decline in the mtDNA in the liver could not be ascertained, and further exploratory studies are needed to clarify the underlying mechanisms.

Limitations of this study include the relatively small sample size and lack of functional assessment of mitochondria. Although we assessed morphological mitochondrial changes by TEM, we did not assess mitochondrial function via mitochondrial membrane

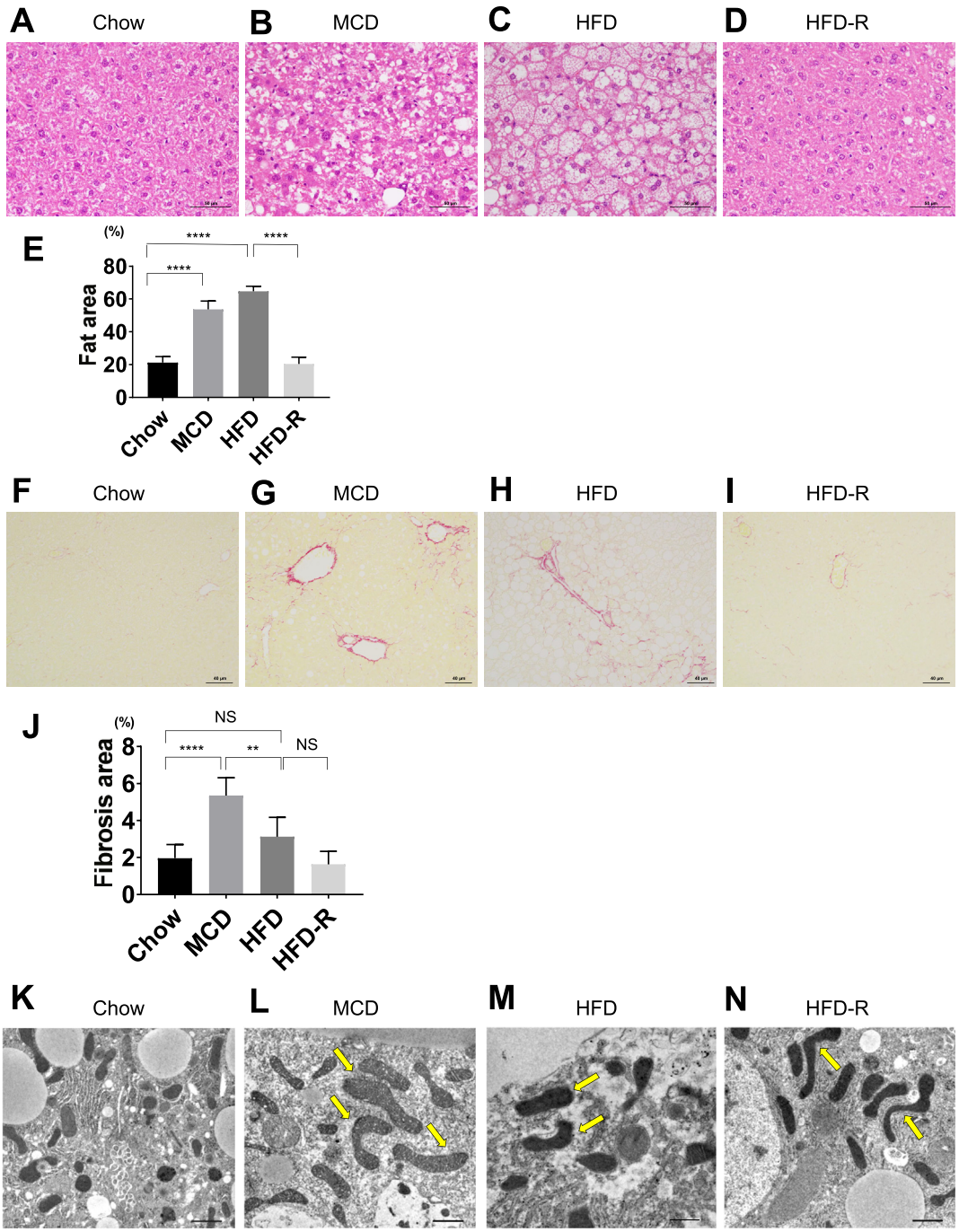

Fig. 2. Impact of diet on the microscopic appearance of the liver
(A–D) Representative liver sections from mice fed different diets for 10 weeks stained with Hematoxylin & Eosin (H&E) (magnification 400 ×). (E) Percentage of fat areas after H&E staining. (F–I) Representative liver sections mice fed different diets for 10 weeks stained with Sirius red (magnification 40 ×). (J) Percentage of fibrotic areas after Sirius red staining (K–N) Ultrastructural changes in mitochondria in the liver. Megamitochondria were identified in the HFD, MCD, and HFD-R group. Scale bar: 1 μm. Results are presented as the means ± SD. *$p < 0.05$, **$p < 0.01$, ***$p < 0.001$, ****$p < 0.0001$. Images are representative of five independent experiments. Intergroup comparison was done by factorial ANOVA followed by Tukey's test. Abbreviations: MCD, methionine/choline-deficient diet; HFD, high-fat diet; HFD-R, high-fat diet recovery; NS, Not Significant. . (For interpretation of the references to colour in this figure legend, the reader is referred to the Web version of this article.)

potential or oxygen consumption rate. These limitations should be addressed in future studies.

In conclusion, the irreversible hepatotoxicity and fibrotic changes with poorer general condition is the feature of MCD-related fatty liver mice model and might be related to the reduced number of mitochondria, while the reversible fat accumulation and body weight gain, along with HFD-induced fatty liver in the HFD mice model may be related to the maintenance of mitochondria number. These results may further indicate that the MCD-induced fatty liver mice model is related to NAFLD with poor hepatic function, including hyponutrition, depression, anorexia, while the HFD-induced NAFLD model may be related to obesity and metabolic syndromes. In summary, our results suggest that the mtDNA copy number can be a biomarker to determine the NAFLD

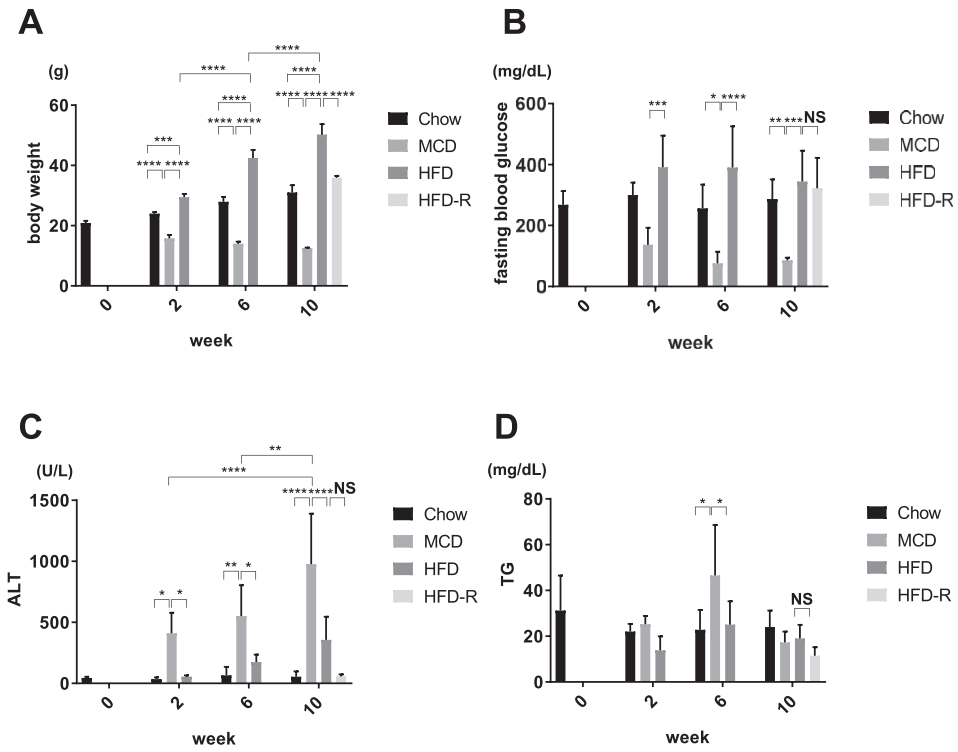

Fig. 3. Effects of different diets on body weight and biochemical test results in mice.
(A) Body weight. (B) Fasting blood glucose. (C) ALT (D) TG. Results are presented as the means ± SD ($n = 4$). Intergroup comparison was done by factorial ANOVA followed by Tukey's test. *$p < 0.05$, **$p < 0.01$, ***$p < 0.001$, ****$p < 0.0001$. Abbreviations: MCD, methionine/choline-deficient diet; HFD, high-fat diet; HFD-R, high-fat diet recovery; ALT, alanine aminotransferase; TG, triglyceride; NS, Not Significant.

type and assess if it is reversible.

Declaration of competing interest

There is no conflict of interest.

Acknowledgments

The authors would like to thank Takao Tsuchida in the Division of Gastroenterology and Hepatology at the Niigata University for the excellent assistance in histological analysis. The authors would also like to thank Nobuyoshi Fujisawa, Yoshitaka Maeda, Kanako Oda, Toshikuni Sasaoka, and all staff members at the Division of Laboratory Animal Resources in Niigata University. The research in the authors' laboratory has been supported in part by Grant-in-Aid for Scientific Research from the Japanese Society for the Promotion of Sciences 25460983 to Kawai H and 20K16983 to Arao Y.

Transparency document

Transparency document related to this article can be found online at https://doi.org/10.1016/j.bbrc.2020.03.180.

Appendix A. Supplementary data

Supplementary data to this article can be found online at https://doi.org/10.1016/j.bbrc.2020.03.180.

Author contributions

YA performed experiments and wrote the manuscript; HK analyzed data and made manuscript revisions; KK made manuscript revisions; TK and ON performed experiments; MH performed experiments; UT supervised the study; ST supervised the study.

References

[1] K.C. Lee, Y.C. Hsieh, Y.Y. Yang, et al., Aliskiren reduces hepatic steatosis and epididymal fat mass and increases skeletal muscle insulin sensitivity in high-fat diet-fed mice, Sci. Rep. 6 (2016) 18899, https://doi.org/10.1038/srep18899.
[2] M.E. Rinella, R.M. Green, The methionine-choline deficient dietary model of steatohepatitis does not exhibit insulin resistance, J. Hepatol. 40 (2004) 47–51, https://doi.org/10.1016/j.jhep.2003.09.020.
[3] H. Itagaki, K. Shimizu, S. Morikawa, et al., Morphological and functional characterization of non-alcoholic fatty liver disease induced by a methionine-choline-deficient diet in C57BL/6 mice, Int. J. Clin. Exp. Pathol. 6 (2013) 2683–2696.
[4] H. Tilg, A.R. Moschen, Evolution of inflammation in nonalcoholic fatty liver disease: the multiple parallel hits hypothesis, Hepatology 52 (2010) 1836–1846, https://doi.org/10.1002/hep.24001.
[5] H.C. Lee, Y.-H. Wei, Oxidative stress, mitochondrial DNA mutation, and apoptosis in aging, Exp. Biol. Med. 232 (2007) 592–606, https://doi.org/10.1177/153537020222700901.
[6] T. Kuznetsova, J. Knez, Peripheral blood mitochondrial DNA and myocardial function, Adv. Exp. Med. Biol. 982 (2017) 347–358, https://doi.org/10.1007/978-3-319-55330-6_19.
[7] M.V. Pinti, G.K. Fink, Q.A. Hathaway, et al., Mitochondrial dysfunction in type 2 diabetes mellitus: an organ-based analysis, Am. J. Physiol. Endocrinol. Metab. 316 (2019) e268–e285, https://doi.org/10.1152/ajpendo.00314.2018.
[8] X. Zhu, Y. Mao, T. Huang, et al., High mitochondrial DNA copy number was associated with an increased gastric cancer risk in a Chinese population, Mol. Carcinog. 56 (2017) 2593–2600, https://doi.org/10.1002/mc.22703.
[9] F. Chiappini, A. Barrier, R. Saffroy, et al., Exploration of global gene expression in human liver steatosis by high-density oligonucleotide microarray, Lab. Invest. 86 (2006) 154–165, https://doi.org/10.1038/labinvest.3700374.
[10] S. Kamfar, S.M. Alavian, M. Houshmand, et al., Liver mitochondrial DNA copy number and deletion levels may contribute to nonalcoholic fatty liver disease susceptibility, Hepat. Mon. 16 (2016), e40774, https://doi.org/10.5812/hepatmon.40774.
[11] S. Sookoian, M.S. Rosselli, C. Gemma, et al., Epigenetic regulation of insulin resistance in nonalcoholic fatty liver disease: impact of liver methylation of

the peroxisome proliferator-activated receptor γ coactivator 1α promoter, Hepatology 52 (2010) 1992–2000, https://doi.org/10.1002/hep.23927.
[12] C.J. Pirola, R. Scian, T.F. Gianotti, et al., Epigenetic modifications in the biology of nonalcoholic fatty liver disease: the role of DNA hydroxymethylation and TET proteins, Medicine (Baltimore) 94 (2015) 1–10, https://doi.org/10.1097/MD.0000000000001480.
[13] H. Ishikawa, A. Takaki, R. Tsuzaki, et al., l-carnitine prevents progression of non-alcoholic steatohepatitis in a mouse model with upregulation of mitochondrial pathway, PLoS One 9 (2014), e100627, https://doi.org/10.1371/journal.pone.0100627.
[14] L. Sun, Z. Fan, J. Chen, et al., Transcriptional repression of SIRT1 by protein inhibitor of activated STAT 4 (PIAS4) in hepatic stellate cells contributes to liver fibrosis, Sci. Rep. 6 (2016) 28432, https://doi.org/10.1038/srep28432.
[15] N. Ghorbanmehr, M. Salehnia, M. Amooshahi, The effects of sodium selenite on mitochondrial DNA copy number and reactive oxygen species levels of in vitro matured mouse oocytes, Cell J 20 (2018) 396–402, https://doi.org/10.22074/cellj.2018.5430.
[16] C.E. Perrone, D.A.L. Mattocks, M. Jarvis-Morar, et al., Methionine restriction effects on mitochondrial biogenesis and aerobic capacity in white adipose tissue, liver, and skeletal muscle of F344 rats, Metabolism 59 (2010) 1000–1011, https://doi.org/10.1016/j.metabol.2009.10.023.